Protected strategy to boost stability of aminated-graphene in Fenton-like reactions

Xu yongsheng[a,1], Dai shuqi[b,1], Li Bin[a], Xia Qing[a], Li Shurong[c], Peng Wenchao[a,*]

[a]School of Chemical Engineering and Technology, Tianjin University, Tianjin 300050, China

[b]South China Advanced Institute for Soft Matter Science and Technology, School of Molecular Science and Engineering, South China University of Technology, Guangzhou 510640, China

[c]Department of Chemistry, College of Chemistry and Chemical Engineering, Xiamen University, Xiamen 361005, China

* Corresponding author:

Peng Wenchao

Tel: 86-22-85356119.

Fax: 86-22-85356119.

E-mail: wenchao.peng@tju.edu.cn.

Number of pages (including the cover page): 40

Number of texts: 4

Number of figures: 27

Number of tables: 7

Contents

Section 1. Materials

The all reagents needed in the experiments were listed in **Table S1**.

Section 2. Methods

Section 2.1 Preparation of GO

The GO was synthesized by modified Hummer's method as follow steps. Firstly, 230 mL concentrated sulfuric acid was stirred in 2 L three-neck flask at 0 ℃. Secondly, 5 g $NaNO_3$ and 5 g graphite are gradually added into above system, respectively. Then, the mixture was stirred constantly and reacted with 30 min. Thirdly, 30 g $KMnO_4$ was added into the reaction system gradually (more than 10 times). After added, the temperature of the system was increased at 35 ℃ and went on the reaction with 30 min. Fifthly, 500 mL deionized water was added into the reaction system gradually. Then, the temperature of system was increased to 98 ℃ and went on the reaction with 60 min. Sixthly, 1200 mL and 500 mL 5 wt% H_2O_2 were added into the system and the solution was filtered at a high temperature. Then, the obtained solid was washed by 5% HCl solution and water, respectively. Finally, the as-prepared sample was dispersed in amount of deionized water and then the suspension stirred with 1 day at room temperature. After that, the suspension was put into dialysis bags and dialysed for five days. The obtained suspension in dialysis bags was GO suspension.

Section 2.2 Preparation of trinuclear iron (III) complex

The preparation process is described as follows:[S1] 27.7 g (50 mmol) of $Fe(NO_3)_3 \cdot 9H_2O$ and 8 ml (100 mmol) of acrylic acid were dissolved in water and then 5.3g (50 mmol) of sodium carbonate were gradually added at room temperature with

stirring. After all the sodium salt had been added, the mixture was stirred for 24 h at room temperature. The trinuclear iron(III) complex (orange solid) was obtained after filtered, washed with deionized water and diethyl ether three times and dried in the vacuum drying oven overnight.

Section 2.3 Preparation of trinuclear cobalt (III) complex

Cobalt(II) carbonate (3 g, 25 mmol) was refluxed with 2.5 ml (40 mmol) of acrylic acid in water for 1 h at 120 ℃. The mixture was filtered and the filtrate was concentrated (rotavap). The solid formed was washed with Et2O and dried in vacuum drying oven overnight.

Section 3. Reaction kinetics calculation

S1.3.1 Catalytic kinetics calculation

In order to evaluate the reaction process, the pseudo-first order reaction rate constant *k* is introduced and the calculation process is shown as equation (S1).

$$-r = kC_A \quad \text{(S1)}$$

Here, C_A is the concentration of phenol in the degradation process. After simplified, the equation (S2) can be obtained from equation (S1).

$$-\ln(\frac{C_A}{C_0}) = kt \quad \text{(S2)}$$

In the equation, C_0 is the initial concentration of phenol, *t* is the reaction time. It is easily seen that the curve of $-\ln(\frac{C_A}{C_0})$ versus *t* is a line and the slope is the value of *k*.

S1.3.2 Deactivation kinetics calculation

As is known to all, for fixed-bed reactor, the design equation can be simplified as follows when the reaction volume is constant.

$$u_0 \frac{dC_{t,z}}{dZ} = r \quad \text{(S3)}$$

Here, u_0 is the speed of peristaltic pump, *Z* is the height of catalyst.

When the phenol oxidation is the pseudo-first order reaction, equation S3 can be simplified as follows when the deactivation of catalyst is not considered.

$$\frac{C_{t,Z}}{C_0} = e^{-\frac{Z \times k}{u_0}} \quad \text{(S4)}$$

To better evaluate the deactivation behavior of the catalyst in the second stage, the deactivation rate constant k_d is introduced and calculated as follows:

According the curve of $\frac{C_{t,Z}}{C_0}$ with reaction time, assuming a zero-order deactivation with respect to time, the deactivation function can be expressed as equation (S5).

$$-\frac{dC_{t,Z}}{dt} = -k_d \quad \text{(S5)}$$

For catalyst/PMS system, the t_d is regarded as the starting time of deactivation period. The equation S4 can be developed into equation S6.

$$\frac{C_{t,Z}}{C_0} = \frac{k_d}{C_0}(t - t_d) + \frac{C_{t_d,Z}}{C_0} \quad \text{(S6)}$$

Here, $C_{t_d,Z}$ is the concentration of phenol in outlet at time t_d. Therefore, if the assumptions above are correct, a plot of $\frac{C_{t,Z}}{C_0}$ versus *t* will give a straight line where the zero-order deactivation rate constant, k_d, can be calculated from the slope.

Section 4. Density functional theory calculation process

The models were computed with density functional theory (DFT) using projected augment wave method[S2] as implemented in the Vienna ab initio Simulation Package(VASP) code. [S3] The generalized gradient approximation (GGA) of Perdew-Burke-Ernzerhof (PBE) is used for the exchange-correlation potential.[S4] Plane-wave basis set was used with an energy cutoff of 500 eV. The convergence criterion for electronic structure iteration was set to be 1×10^{-4} eV and structural optimization would be terminated until all forces were smaller than 0.05eV/Å. Polarization effect was considered. The charge transfer was analyzed by calculating the charge density using the Bader charge analysis method.[S5,6] K-meshs was set as 1×1×1 in this work. The visualization and plotting was gained by The Visualization for Electronic and Structural Analysis (VESTA)[S7]

software

The adsorption energy was defined as:

$$E_{ads} = E_{cluster+PMS} - E_{cluster} - E_{PMS}$$

Where $E_{cluster+PMS}$ was the total energy of the model, $E_{cluster}$ was the energy of the cluster model, E_{PMS} was the energy of free PMS.

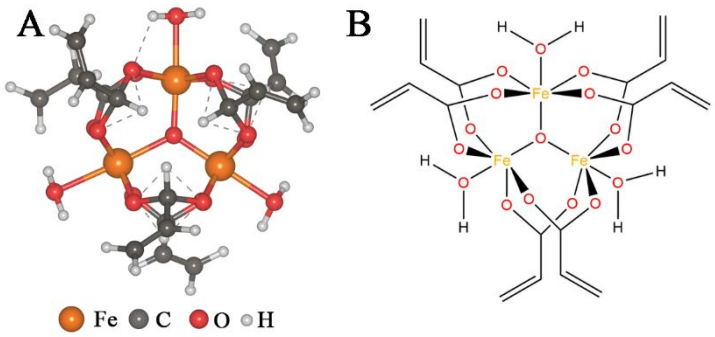

Figure S1. (A) Ball-and-stick model of unit structure for Fe_3 cluster; (B) Structural formula of unit structure for Fe_3 cluster.

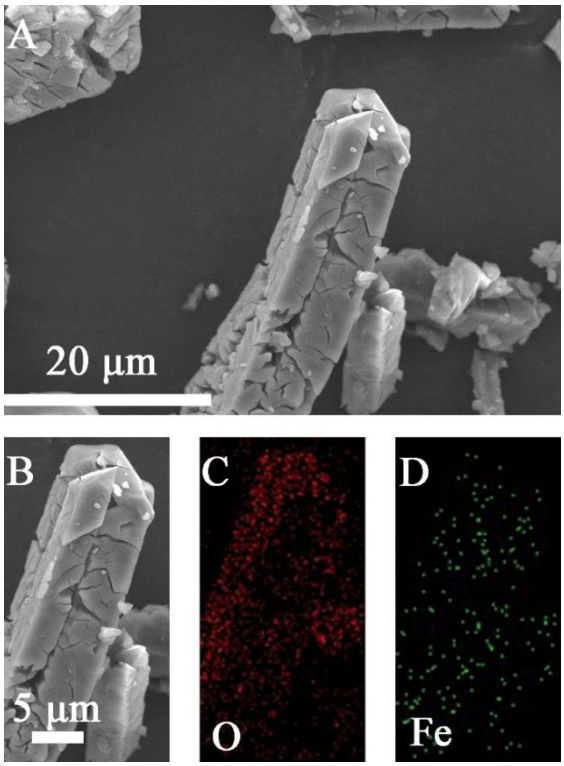

Figure S2. SEM images of Fe_3 cluster at 20 μm (A) and 5 μm (B); EDS mapping of Fe_3 cluster about O (C) and Fe (D) elements.

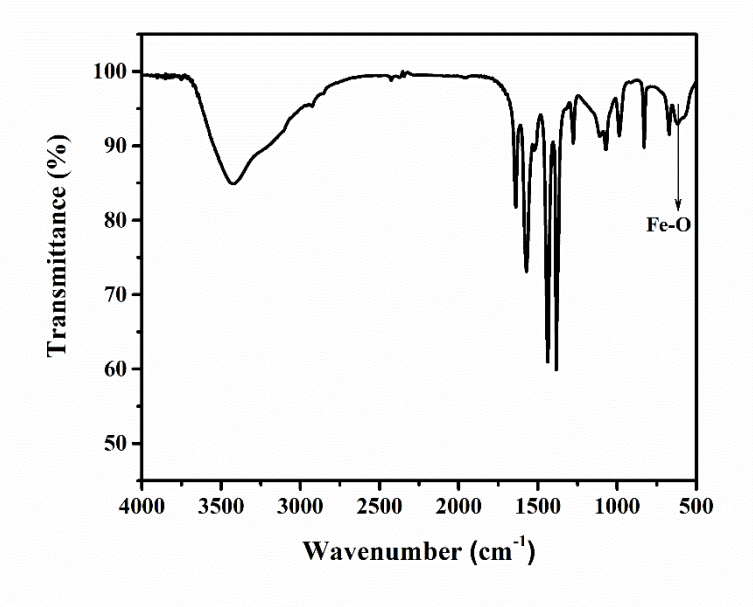

Figure S3. FTIR spectrum of Fe_3 cluster.

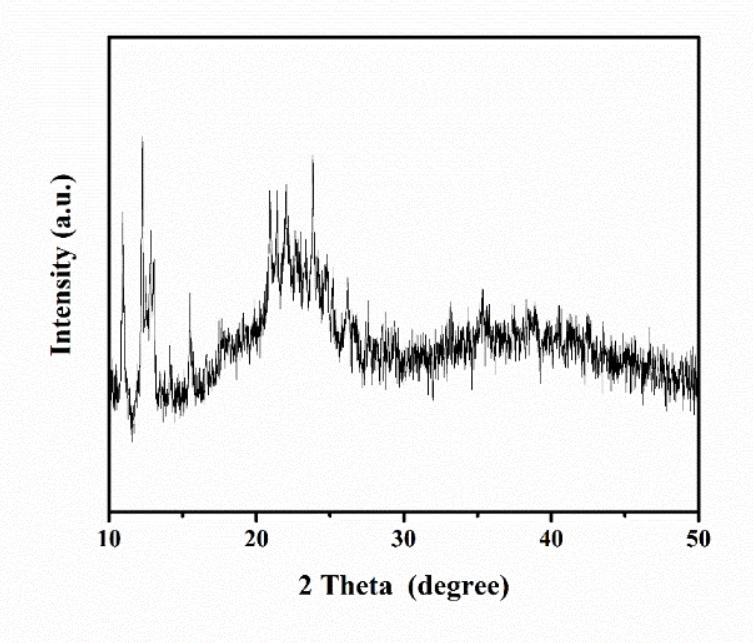

Figure S4. XRD pattern of Fe_3 cluster.

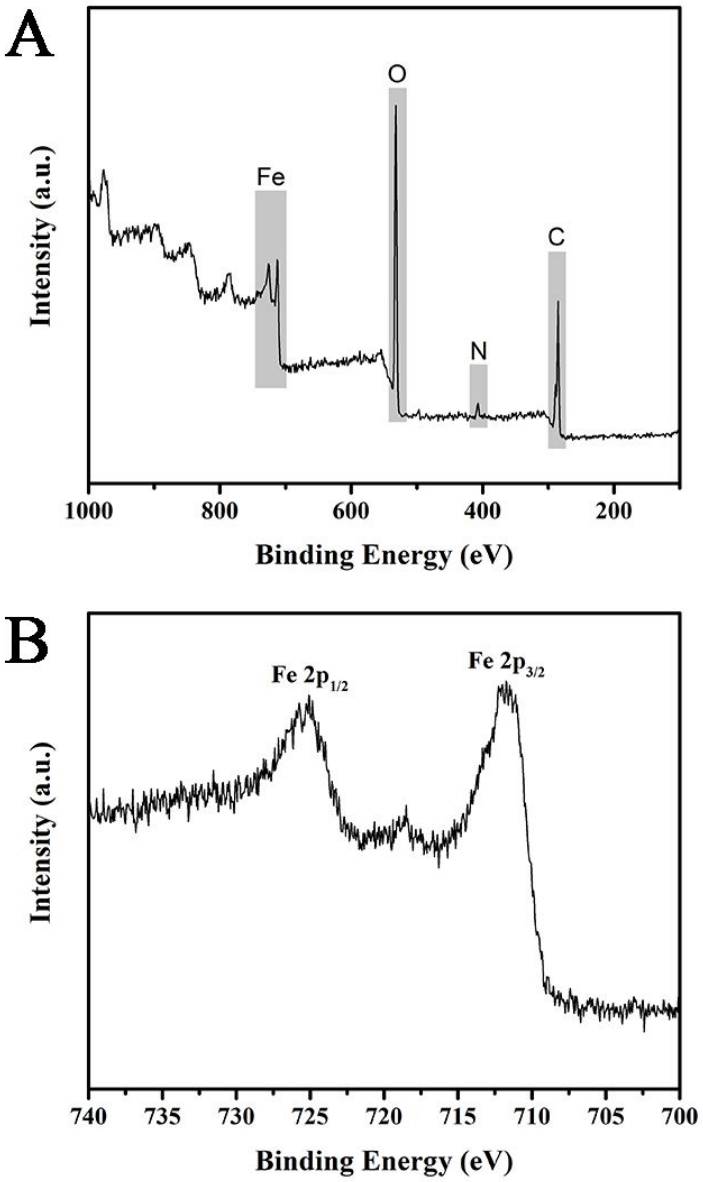

Figure S5. XPS survey spectrum of Fe_3 cluster (A) and XPS spectrum of Fe in the Fe_3 cluster (B).

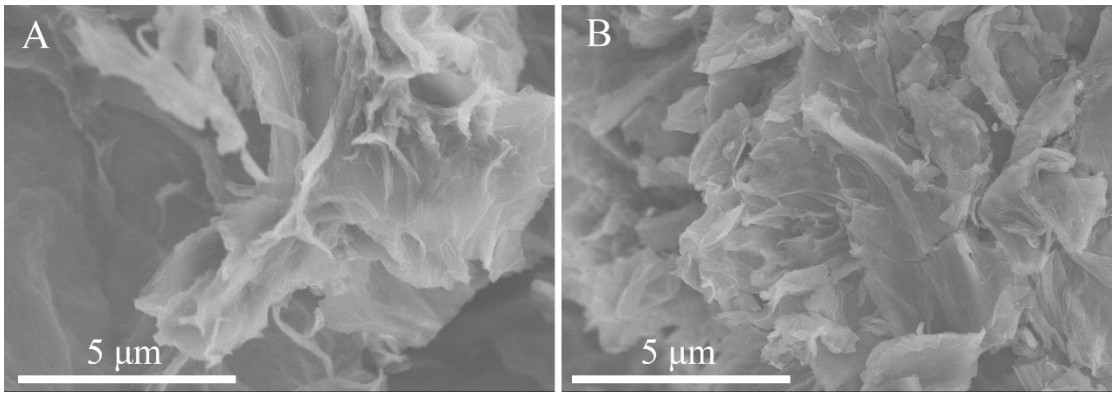

Figure S6. SEM images of NH_2-GR (A) and Fe_3-NH_2-GR (B).

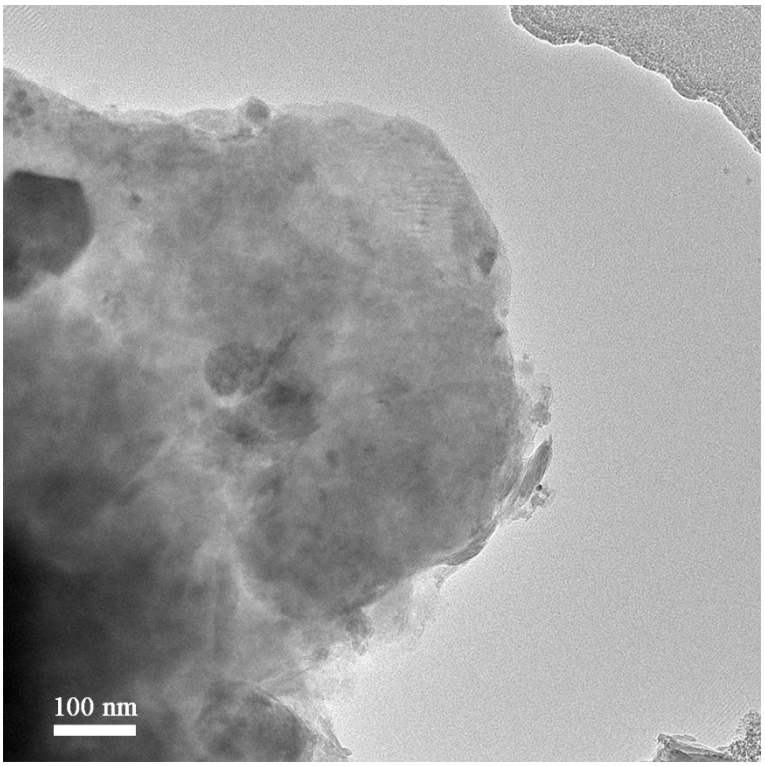

Figure S7. TEM image of NH_2-GR.

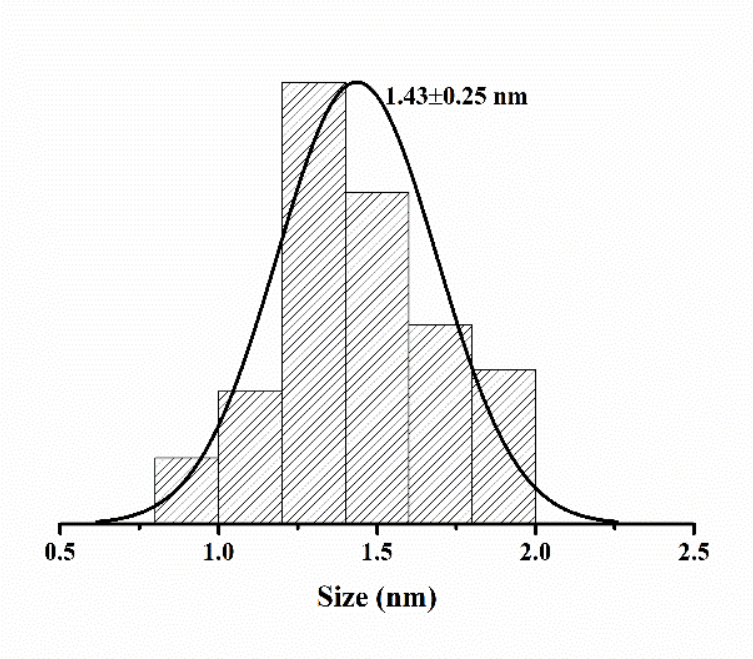

Figure S8. Particle size distribution diagram of Fe_3 cluster on the Fe_3-NH_2-GR.

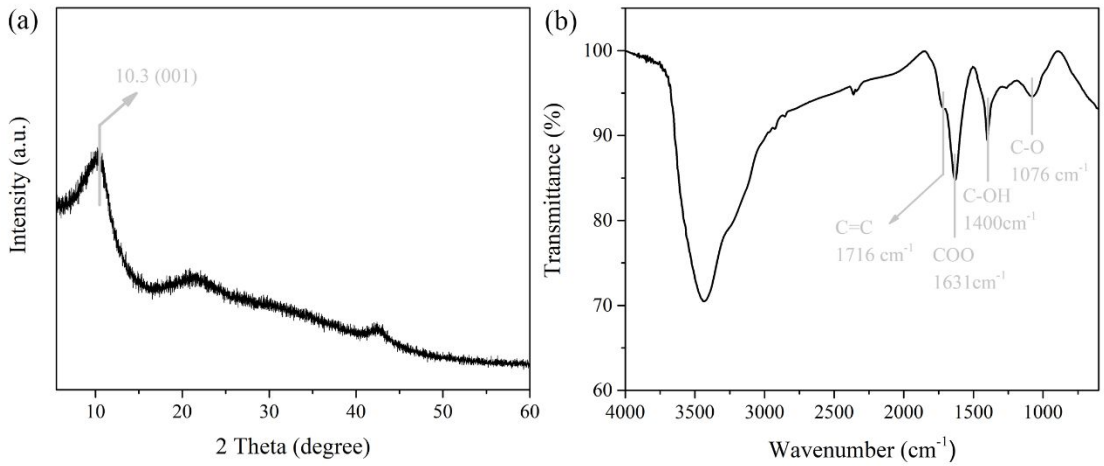

Figure S9. XRD pattern (a) and FTIR spectrum (b) of GO.

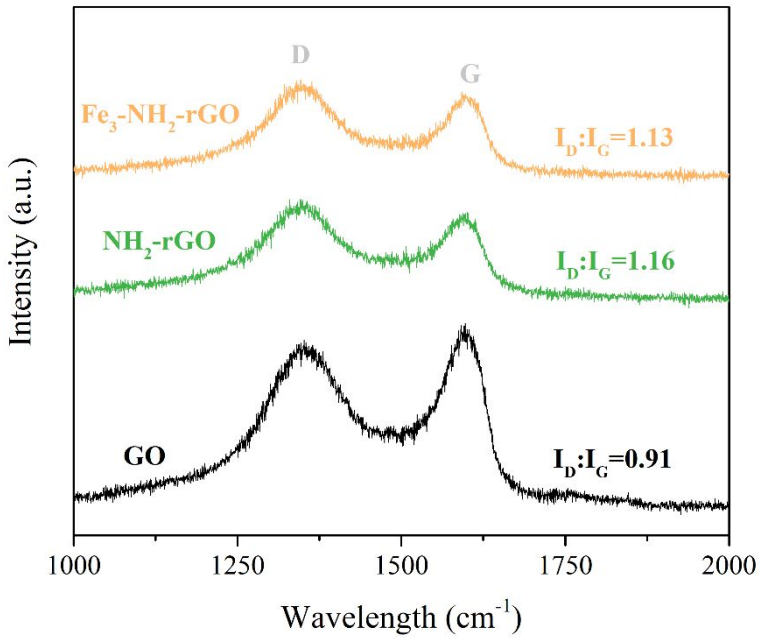

Figure S10. Raman spectra of materials.

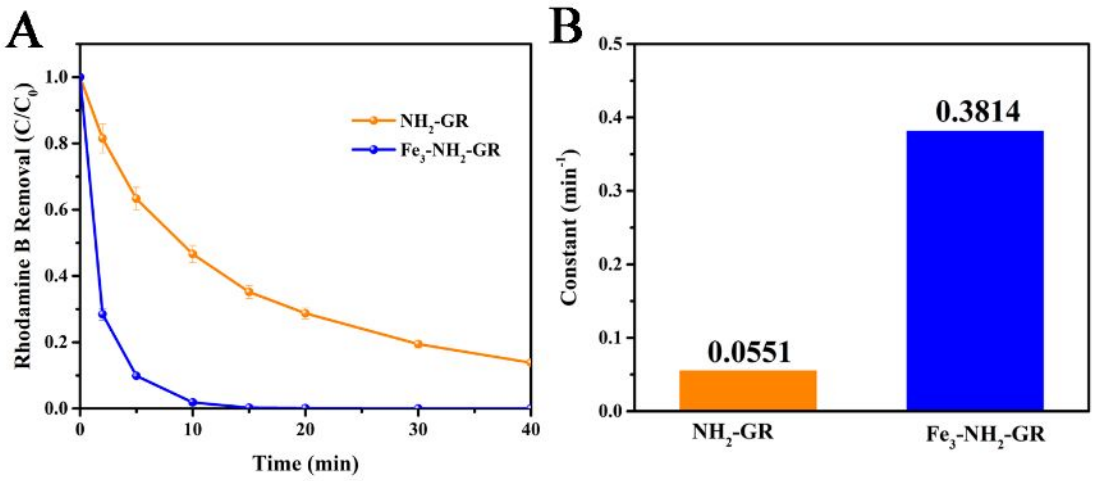

Figure S11. (A) Rhodamine B degradation process of Fe_3-NH_2-GR and NH_2-GR in stirred reactor; (B) Reaction constants for Fe_3-NH_2-GR and NH_2-GR in rhodamine B degradation.

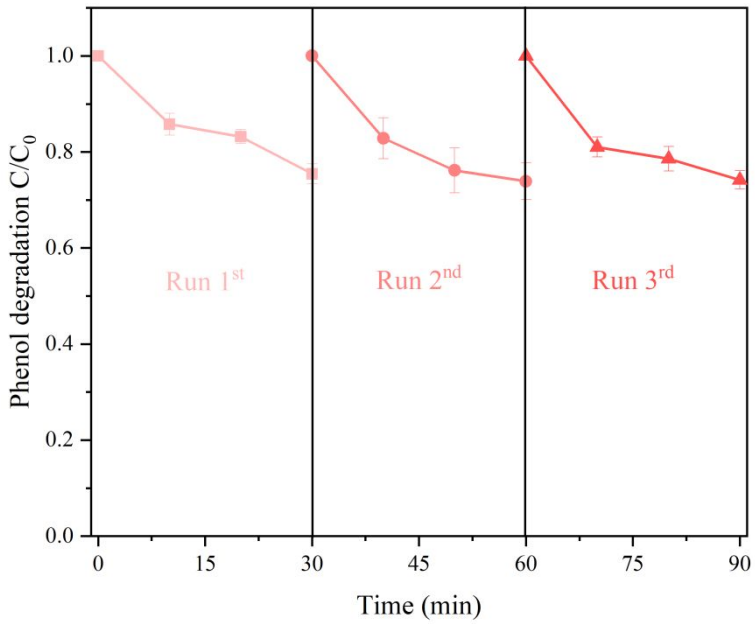

Figure S12. Stability tests of used Fe_3-NH_2-GR after fixed bed reactor experiment. Conditions: C(phenol)= 10 mg/L; C(Catalyst)= 500 mg/L; C(PMS)=1000 mg/L.

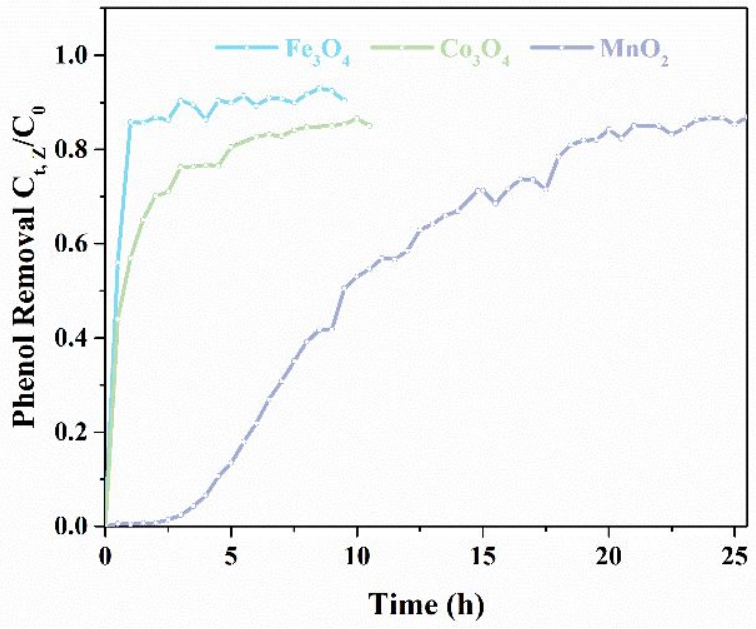

Figure S13. Stabilities of Fe_3O_4, Co_3O_4 and MnO_2 in phenol degradation with fixed bed reactor.

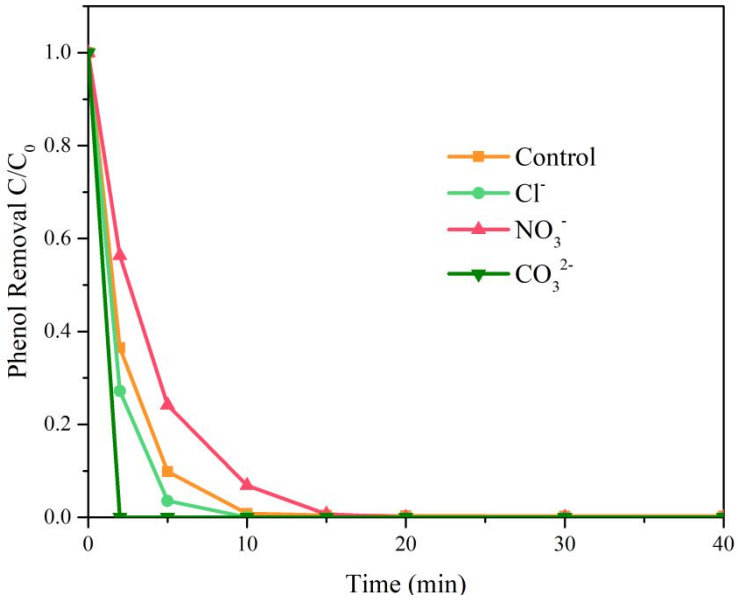

Figure S14. Degradation system with different ions in stirred reactor. Conditions: C(phenol)= 20 mg/L; C(Catalyst)= 100 mg/L; C(PMS)=1000 mg/L; C(anions)=10 mM.

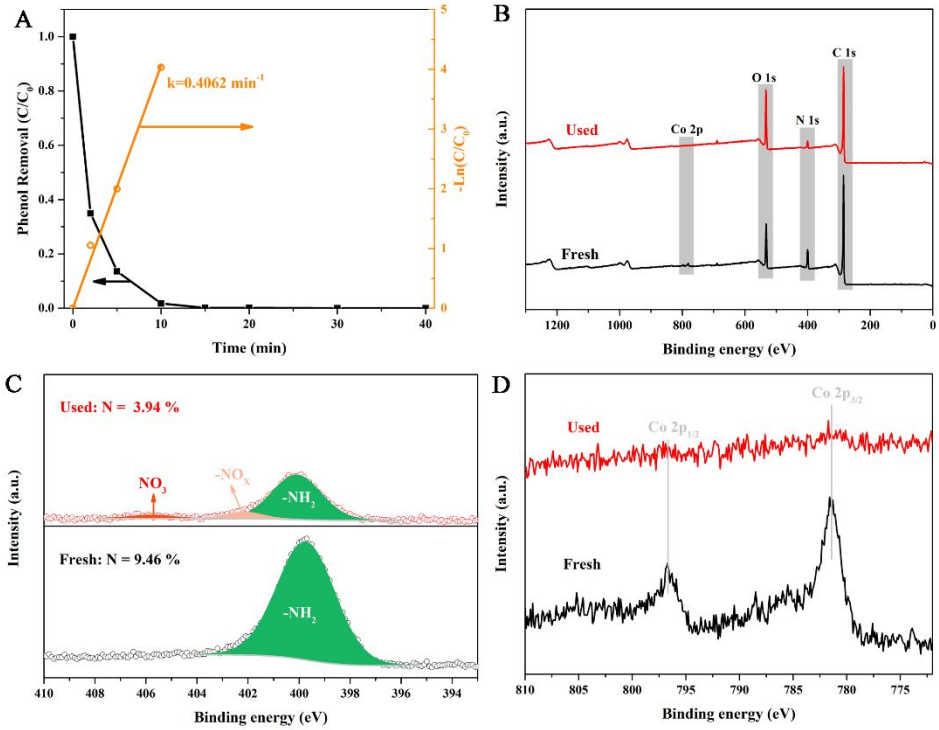

Figure S15. (A) Phenol degradation process with (Co3-NH2-GR+PMS). Conditions: C(phenol)= 20 mg/L; C(Catalyst)= 150 mg/L; C(PMS)=1000 mg/L. (B) XPS survey spectra of Co3-NH2-GR before and after use. (C) N 1s spectra of Co3-NH2-GR before and after use. (D) Co 2p spectra of Co3-NH2-GR before and after use.

Note: Then Co_3-NH_2-GR is synthesized using the same method as Fe_3-NH_2-GR. As shown in **Figure R1A**, 100% phenol is degraded within 15 min and the reaction rate constant can reach 0.4 min^{-1}. But from the XPS survey and N 1s spectra of Co_3-NH_2-GR before and after use (**Figure R1B~C**), the N content decreases obviously after use. Although the activity of Co_3-NH_2-GR is still enhanced compared with NH_2-GR, Co_3 cluster doesn't have the similar protection function to decrease the loss of N in the NH_2-GR. The Co 2p spectra is therefore investigated further in **Figure R1D**. Obviously, the Co content decreases rapidly, illustrating that Co cannot bond with -NH_2 firmly. The leaded Co may be important active sites for PMS activation. Furthermore, the Co is a toxic element, which will cause secondary pollution easily. Therefore, we select Fe_3 cluster as the protective agent finally.

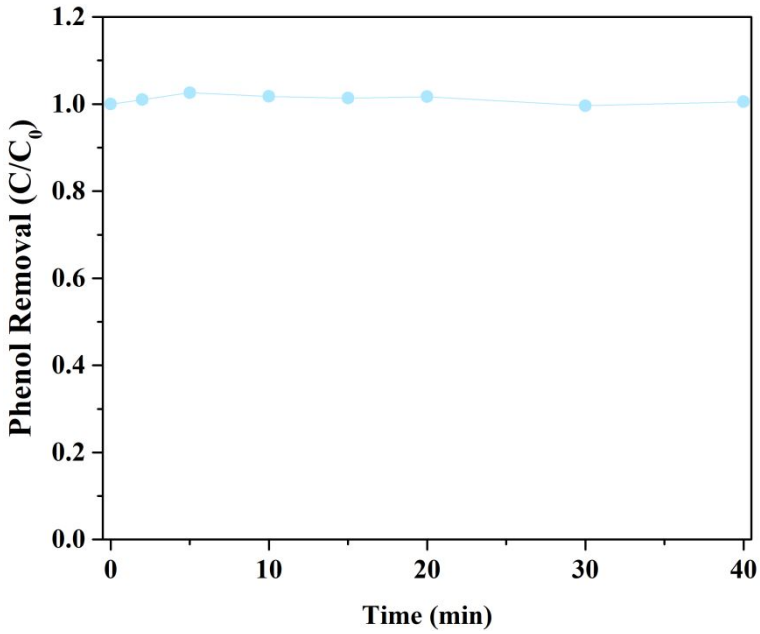

Figure S16. Phenol degradation of Fe_3 Cluster. Conditions: C(phenol)= 20 mg/L; C(Catalyst)= 100 mg/L; C(PMS)=1000 mg/L.

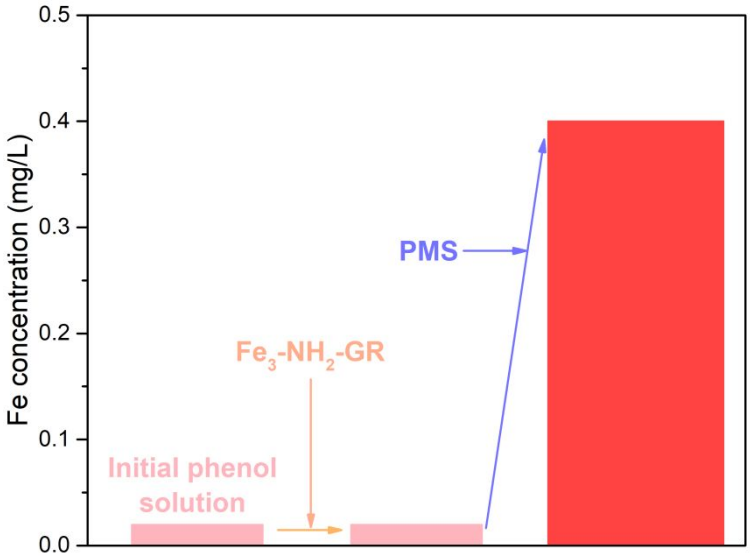

Figure S17. Concentration of Fe in the phenol solution with (Fe_3-NH_2-GR+PMS).

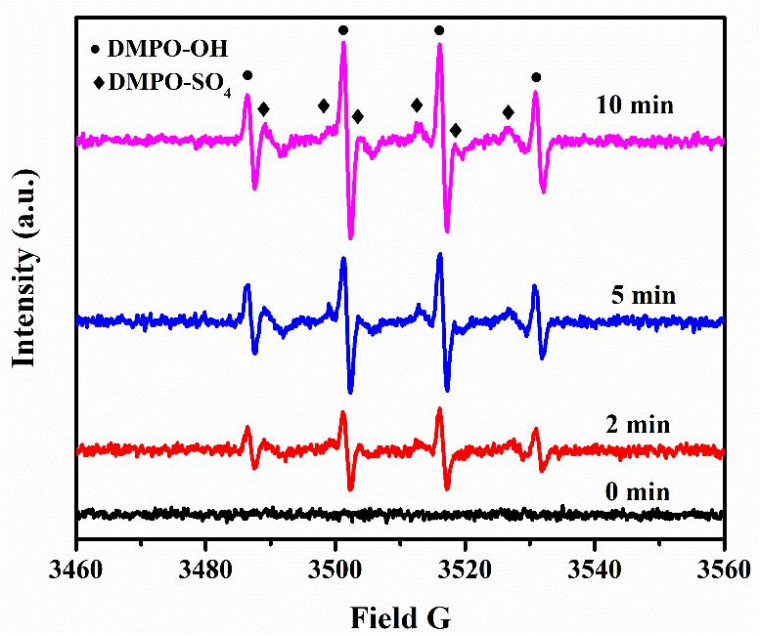

Figure S18. EPR spectra of ·OH and $SO_4^{\cdot-}$ with NH_2-GR at different reaction time.

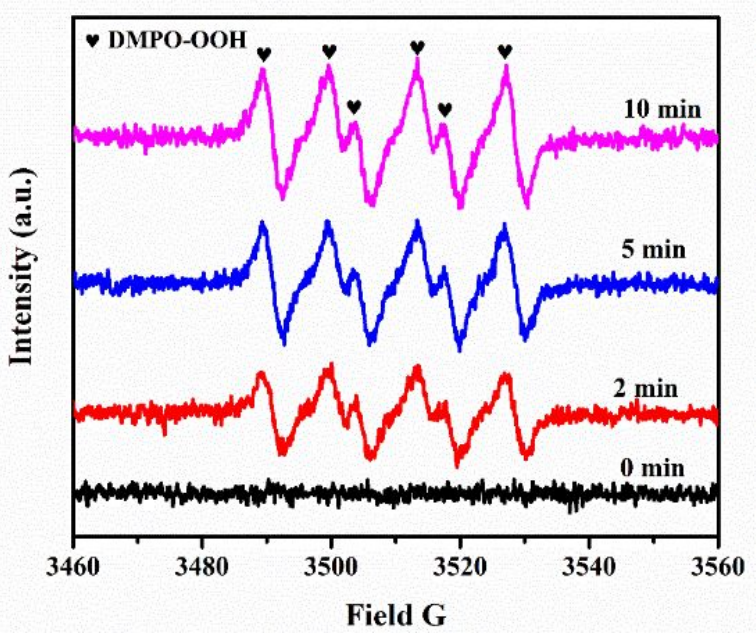

Figure S19. EPR spectra of $O_2^{\bullet-}$ with NH_2-GR at different reaction time.

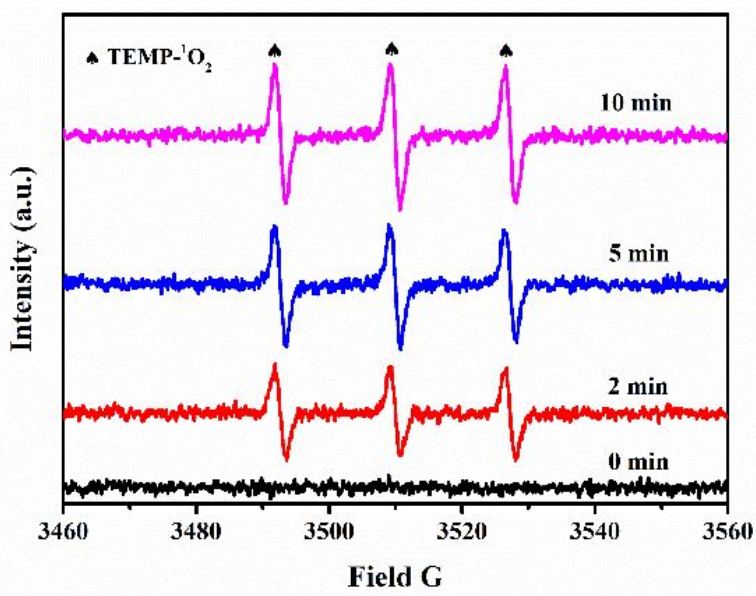

Figure S20. EPR spectra of $^1O_2$ with NH_2-GR at different reaction time.

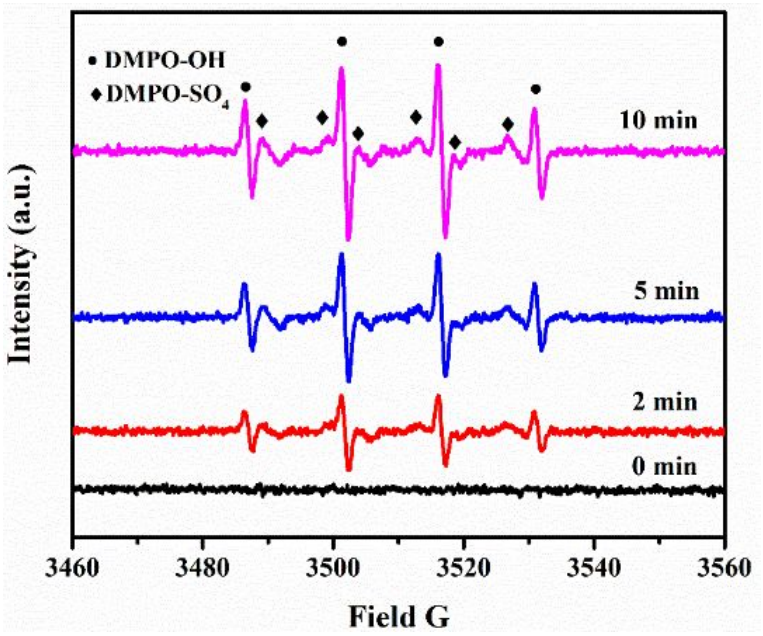

Figure S21. EPR spectra of ·OH and $SO_4^{\cdot-}$ with Fe_3-NH_2-GR at different reaction time.

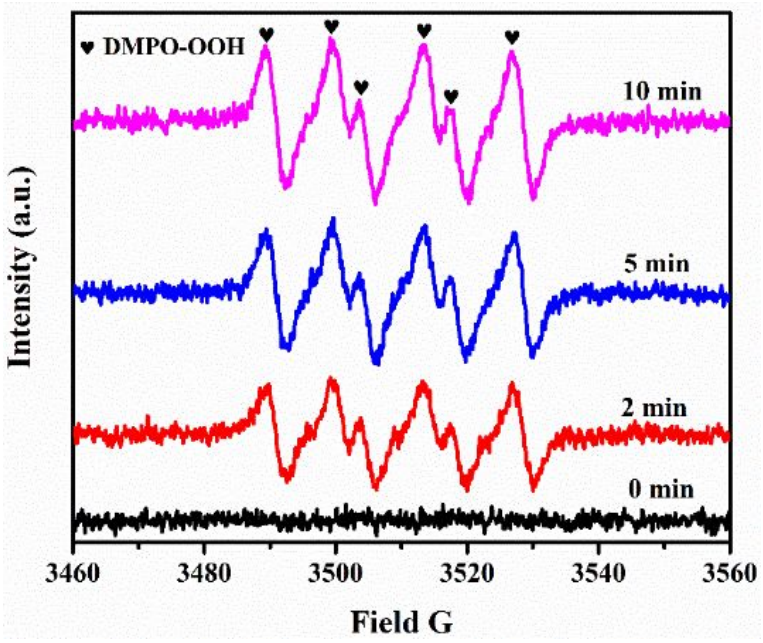

Figure S22. EPR spectra of $O_2^{\bullet-}$ with Fe_3-NH_2-GR at different reaction time.

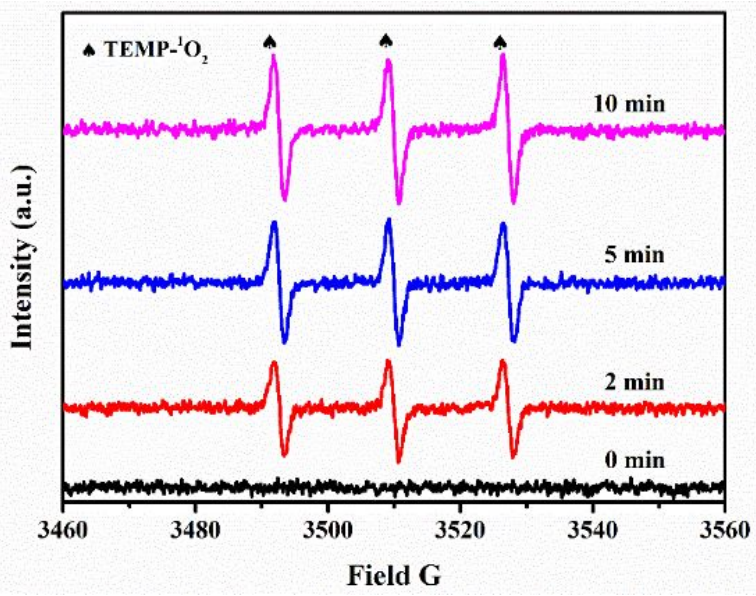

Figure S23. EPR spectra of $^1O_2$ with Fe_3-NH_2-GR at different reaction time.

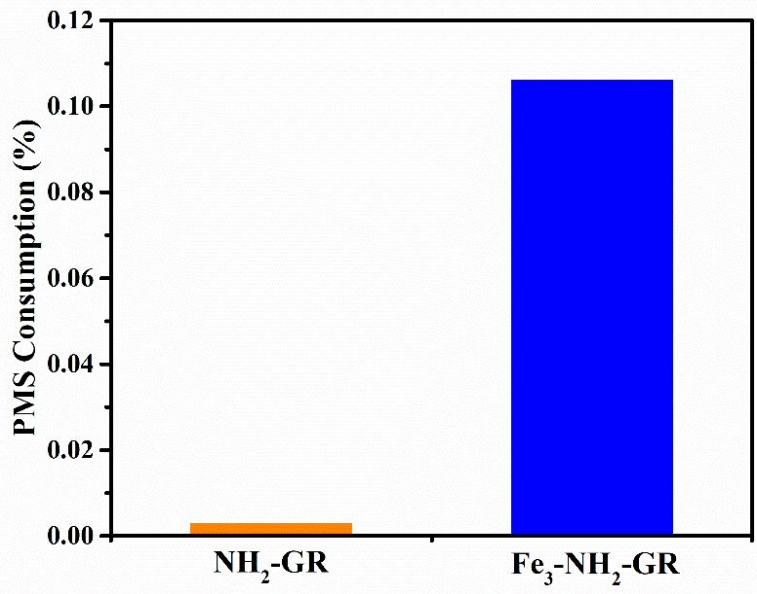

Figure S24. PMS consumption during 5 minutes for NH_2-GR and Fe_3-NH2-GR.

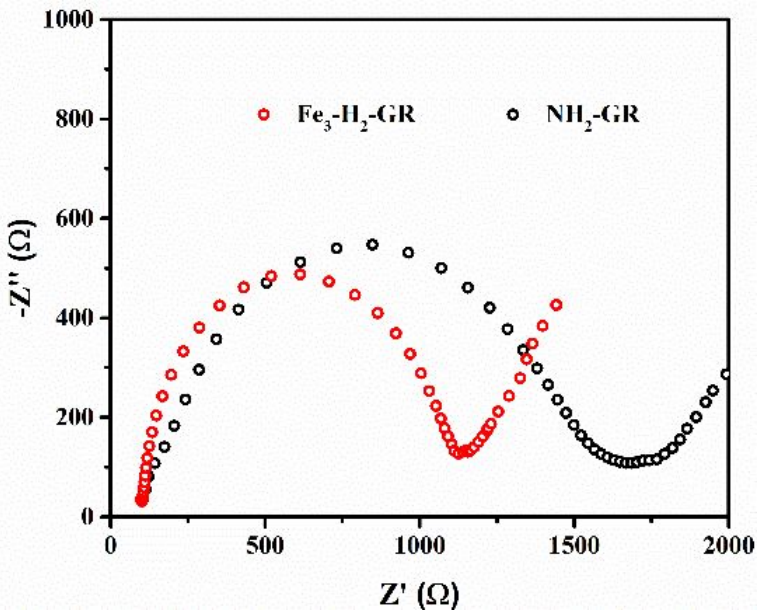

Figure S25. EIS Nyquist plots of NH_2-GR and Fe_3-NH_2-GR with the existence of PMS and phenol.

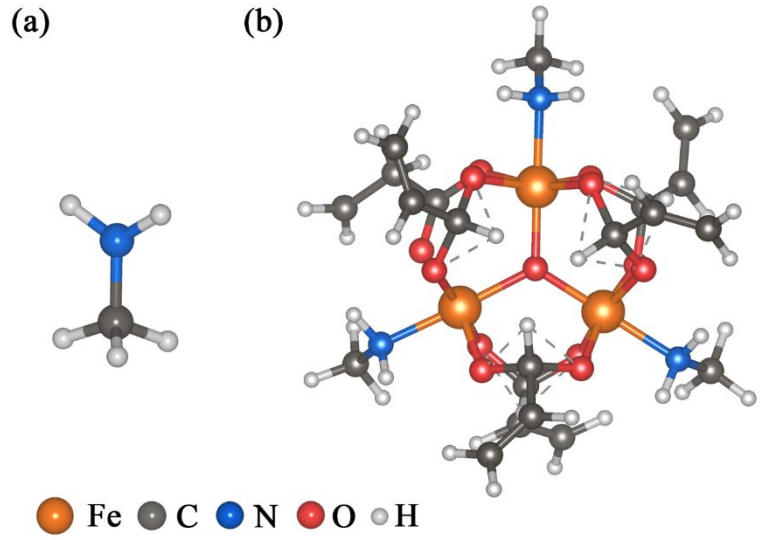

Figure S26. Ball-and-stick models of model 1 (a) and 2 (b).

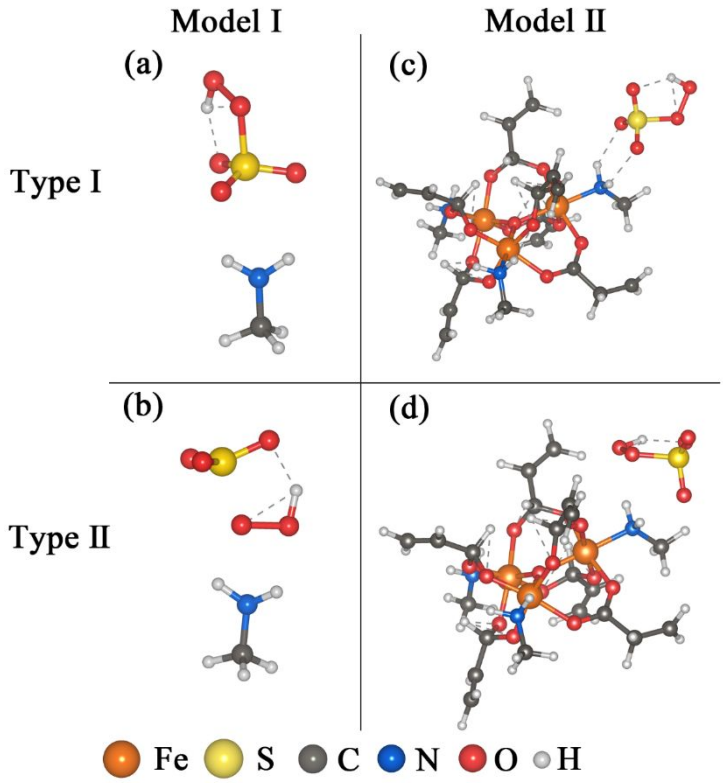

Figure S27. PMS adsorption on different models with different types.

Table S1. Reagents used in the experiments.

Chemical name	CAS no.	Mass fraction	Sources
Phenol	108-95-2	99.0 %	Fuchen Chemical Reagents Co., Ltd. Tianjin, China
Rhodamine B	81-88-9	99.0%	Chemart Chemical Technology Co., Ltd. Tianjin, China
Ferroferric oxide	1317-61-9	95.0%	Heowns Biochemical Technology Co., Ltd. Tianjin, China
Cobaltosic oxide	1308-06-1	95.0%	Heowns Biochemical Technology Co., Ltd. Tianjin, China
Manganese dioxide	1313-13-9	99.0%	Heowns Biochemical Technology Co., Ltd. Tianjin, China
Potassium peroxomonosulfate	37222-66-5	(4.5%) active oxygen	Macklin Biochemical Co., Ltd. Shanghai, China
Ethylenediamine	107-15-3	99.0 %	Aladdin Industrial Co., Ltd. Shanghai, China
Methanol	67-56-1	99.9 %	Kermel Chemical Reagents Co., Ltd. Tianjin, China
Graphite	7782-42-5	/	Aladdin Industrial Co., Ltd. Shanghai, China
Potassium permanganate	7722-64-7	99.5 %	Yuanli Chemical Reagents Co., Ltd. Tianjin, China
Sodium nitrate	7631-99-4	99.0 %	Yuanli Chemical Reagents Co., Ltd. Tianjin, China
Concentrated sulfuric acid	7664-93-9	98.0 %	Yuanli Chemical Reagents Co., Ltd. Tianjin, China
Deionized Water	7732-18-5	/	Nankai Chemical Reagents Co., Ltd. Tianjin, China
p-Benzoquinone	106-51-4	99%	Adamas Reagent, Co., Ltd. Shanghai, China
Tert-butanol	75-65-0	99.5%	Kermel Chemical Reagents Co., Ltd. Tianjin, China
Furfuryl alcohol	98-00-0	99.0%	Adamas Reagent, Co., Ltd. Shanghai, China

Table S2. Detection conditions for organics in HPLC.

Materials	Mobile phase (volume ratio)			Flow rate (mL/min)	Detection wavelength (nm)
	Acetonitrile	Water	Methanol		
phenol	40	60	/	1	220
rhodamine B	/	75	25	1	550

Table S3. Detailed Mössbauer parameters (corresponding to Fig. 1A)

Materials	Assignment	IS (mm/s)	QS (mm/s)	Spectral contribution (%)
Fe_3-NH_2-GR	Fe-N	0.51	0.82	16.9
	Fe-O	0.32	0.76	83.1

Table S4. Activity comparison between Fe_3-NH_2-GR and other graphene-based catalysts**.**

Materials	Pollutants	Catalyst concentration	Reaction rate constant	Ref
Fe_3-NH_2-GR	Phenol (20 mg/L)	0.1 $g \cdot L^{-1}$	0.48	This work
NH_2-GR	Phenol (20 mg/L)	0.1 $g \cdot L^{-1}$	0.03	This work
NG-700	Phenol (20 mg/L)	0.1 $g \cdot L^{-1}$	0.11	3
P-NRGO	Phenol (50 mg/L)	0.05 $g \cdot L^{-1}$	0.35	9
ANGH	Phenol (20 mg/L)	0.2 $g \cdot L^{-1}$	0.61	16
N-rGO	Sulfachloropyridazine (20 mg/L)	0.2 $g \cdot L^{-1}$	0.032	S8
N-rGO-air	Phenol (20 mg/L)	0.4 $g \cdot L^{-1}$	0.40	S9
N-RGO	Bisphenol A (0.385 mmol/L)	0.12 $g \cdot L^{-1}$	0.71	S10
SNG-0.3	Phenol (20 mg/L)	0.2 $g \cdot L^{-1}$	0.04	S11
rGO-NS	Methyl paraben (20 mg/L)	0.4 $g \cdot L^{-1}$	0.35	S12

Table S5. Parameters of deactivation for common metal oxides.

Metal oxide	Useful time (h)	Fast deactivation			Slow deactivation		
		Period (h)	Equation	Constant ($mg \cdot L^{-1} \cdot h^{-1}$)	Period (h)	Equation	Constant ($mg \cdot L^{-1} \cdot h^{-1}$)
Fe_3O_4	/	0~1	y=0.9102t	9.102	1~9.5	y=0.0071x+0.857	0.071
Co_3O_4	/	0~3	y=0.3178x	3.178	3~10.5	y=0.0144x+0.713	0.144
MnO_2	3.5	4~9.5	y=0.0777x-0.244	0.777	20~25.5	y=0.0059x+0.715	0.059
		9.5~20	y=0.0306x+0.230	0.306			

Table S6. N 1s spectra analysis of Fe_3-NH_2-GR and NH_2-GR before and after reaction.

Material		N content (at%)	-NH_2		-O-NO_2		-NO_X	
			Binding energy (eV)	Content (%)	Binding energy (eV)	Content (%)	Binding energy (eV)	Content (%)
NH_2-GR	Before reaction	9.28	399.68	100	/	/	/	/
	After reaction	4.82	399.88	88	/	/	402.40	12
Fe_3-NH_2-GR	Before reaction	6.52	399.90	100	/	/	/	/
	After reaction	7.12	400.25	66	408.10	34	/	/

Table S6. Adsorption energies of different types between PMS and two models.

E_{ads} (eV)	Model Ⅰ	Model Ⅱ
Type Ⅰ	-0.311705	-0.835808
Type Ⅱ	-0.274902	-0.726118

References

[S1] G. Losada, M. A. Mendiola, M. T. Sevilla, *Inorg. Chim. Acta* **1997**, *255*, 125–131.

[S2] P.E. Blöchl, Projector augmented-wave method, Phys. Rev. B 50 (1994) 17953-17979.

[S3] G. Kresse, J. Furthmuller, Efficient iterative schemes for ab initio total-energy calculations using a plane-wave basis set, Phys. Rev. B 54 (1996) 11169-11186.

[S4] J.P. Perdew, K. Burke, M. Ernzerhof, Generalized gradient approximation made simple, Phys. Rev. Lett. 77 (1996) 3865-3868.

[S5] R.F.W. Bader, Atoms in Molecules: A Quantum Theory, Clarendon Press1994.

[S6] W. Tang, E. Sanville, G. Henkelman, A grid-based Bader analysis algorithm without lattice bias, J. Phys.: Condensed Matter 21 (2009) 084204.

[S7] K. Momma and F. Izumi, "VESTA 3 for three-dimensional visualization of crystal, volumetric and morphology data," J. Appl. Crystallogr., 44, 1272-1276 (2011).

[S8] Kang, J.; Duan, X.; Zhou, L.; Sun, H.; Tadé, M. O.; Wang, S., Carbocatalytic activation of persulfate for removal of antibiotics in water solutions. Chem. Eng. J. 2016, 288, 399-405.

[S9] Li, D.; Duan, X.; Sun, H.; Kang, J.; Zhang, H.; Tade, M. O.; Wang, S., Facile synthesis of nitrogen-doped graphene via low-temperature pyrolysis: The effects of precursors and annealing ambience on metal-free catalytic oxidation. Carbon 2017, 115, 649-658.

[S10] Wang, X.; Qin, Y.; Zhu, L.; Tang, H., Nitrogen-Doped Reduced Graphene Oxide as a Bifunctional Material for Removing Bisphenols: Synergistic Effect between Adsorption and Catalysis. Environ. Sci. Technol. 2015, 49 (11), 6855-6864.

[S11] Duan, X., O'Donnell, K., Sun, H., Wang, Y. and Wang, S., Sulfur and Nitrogen Co-Doped Graphene for Metal-Free Catalytic Oxidation Reactions. Small, 2015, 11, 3036-3044.

[S12] Sun, P.; Liu, H.; Feng, M.; Guo, L.; Zhai, Z.; Fang, Y.; Zhang, X.; Sharma, V. K., Nitrogen-sulfur co-doped industrial graphene as an efficient peroxymonosulfate activator: Singlet oxygen-dominated catalytic degradation of organic contaminants. Appl. Catal., B 2019, 251, 335-345.